

Ultrasonic vibration assisted grinding of bio-ceramic materials: an experimental study on edge chippings with Hertzian indentation tests

Hayelom D. Tesfay¹ · Zhigang Xu² · Z. C. Li³

Received: 13 September 2015 / Accepted: 29 December 2015 / Published online: 15 February 2016
© Springer-Verlag London 2016

Abstract Bio-ceramics are biocompatible ceramic materials that are widely used for biomedical engineering applications due to their excellent properties. Because of their inherent hardness and brittleness properties, bio-ceramics are difficult to machine. Abrasive machining such as diamond grinding is one of the most widely used machining for bio-ceramic materials. However, one of the key technical challenges resulted from grinding is edge chipping. The presence of edge chipping in a workpiece affects its dimensional accuracy, machining cost, and potential service time. It is, therefore, crucial to develop a new cost-effective manufacturing process relevant to control edge chipping in diamond grinding of bio-ceramics. In this paper, an ultrasonic vibration-assisted grinding (UVAG) system is developed to investigate the effect of ultrasonic vibration on edge chippings. Hertzian indentation tests are also conducted to validate the experimental results. Results reveal that edge chipping of bio-ceramic materials can be reduced significantly with the assistance of ultrasonic vibration. The results of this study can be applied to other manufacturing process when edge chippings of brittle materials are expected to be controlled.

Keywords Bio-ceramics · Edge chipping · Grinding · Hertzian indentation · Machining · Surface quality · Ultrasonic vibration

1 Introduction

Bio-ceramics are class of ceramics that are designed to repair and replace diseased or damaged parts or functions of the human body in a safe, reliable, and economic manner [1–6]. Superior properties of bio-ceramic materials, such as high strength, chemical stability, good biocompatibility, and high wear resistance, make them attractive for medical applications [7]. Nowadays, bio-ceramics are widely used for replacing hips, knees, teeth, tendons, ligaments, and maxillofacial reconstruction [2, 5, 6]. Typical applications of bio-ceramic materials are illustrated in Fig. 1. They are also used in the form of bulk or porous materials with a specific shape such as implant, prostheses, or prosthetic devices. Other applications of bio-ceramics include dental restorations for implants, augmentation and stabilization of the jaw bone, and bone fillers, etc. [2]. Moreover, bio-ceramics provide less wear rate of the implant polyethylene components and produce negligible amount of metal ion release [8].

Compared to metals and polymers, bio-ceramics have been considered as one of the most important materials in biomedical engineering applications due to their superior physical and mechanical properties [2, 9]. However, these exceptional properties also bring serious drawbacks, which limit their wider applications, especially on clinical performance [10]. The main drawback of bio-ceramic materials is their inherent brittleness, resulting in high fracture rates in clinical trials [11–13]. For instance, the performance of the experimental core ceramic in posterior fixed partial dentures shows a 7 % fracture rate after 2 years' service [14]. Due to their brittleness,

✉ Z. C. Li
zli@ncat.edu

¹ Department of Computational Science and Engineering, North Carolina Agricultural and Technical State University, Greensboro, NC 27411, USA

² Department of Mechanical Engineering, North Carolina Agricultural and Technical State University, Greensboro, NC 27411, USA

³ Department of Industrial and Systems Engineering, North Carolina Agricultural and Technical State University, Greensboro, NC 27411, USA

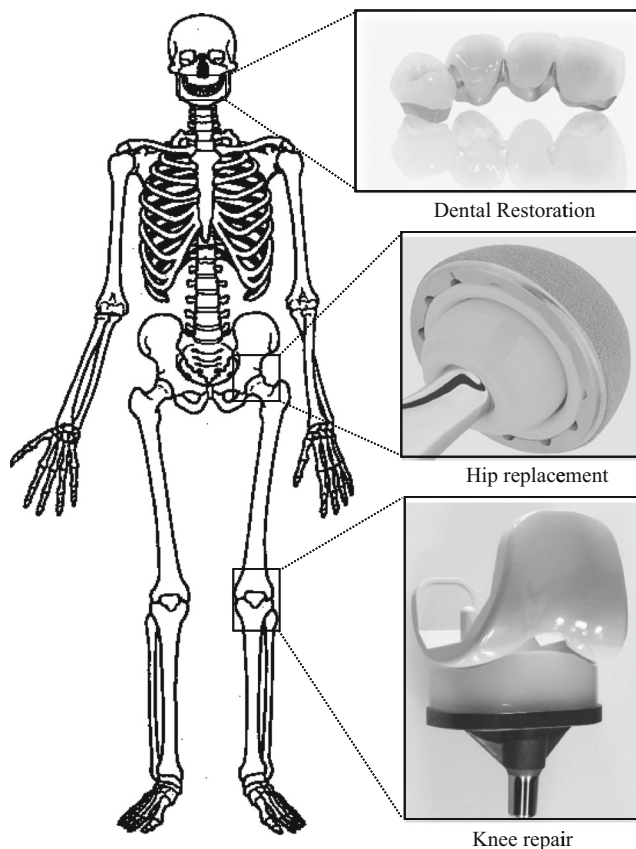


Fig. 1 Application of bio-ceramic in different fields: dental restoration, hip replacement, and knee repair

bio-ceramics are sensitive to stress concentrations around pre-existing cracks, leading them to have low fracture toughness compared to metals [11]. Research indicates that dental crowns fail at a rate of about 3 % each year due to surface and subsurface damages resulted from abrasive machining [15]. Likewise, bio-ceramics are very difficult to machine to desired shape and accuracy due to their hardness, mechanical strength, and chemical inertness properties [16].

Abrasive machining processes such as diamond grinding is one of the most important operations employed to machine bio-ceramics [15]. However, the principal technical challenge resulted from diamond grinding is edge chipping, which is a typical surface damage phenomenon commonly observed during the machining of brittle materials [17]. The presence of edge chipping not only affects their dimensional and geometric accuracy but also causes severe potential failure of the ceramic components during service due to the cracks left on the machined surface [18]. Chai et al. [19] reported that edge chippings are the most frequent fracture modes in teeth, which can lead to deterioration and ultimate loss of tooth function and degradation of tooth enamel [20]. One solution to be considered to reduce (or eliminate) machining-induced edge chippings is to develop new types of machining processes, equipment, and tools [2, 8].

Many researchers have reported studies on edge chippings. Ng et al. [17] and Cao [21] described three kinds of edge chipping when grinding glass ceramics, namely, entry edge chipping (the tool initially contacts the workpiece), interior edge chipping (due to the brittle nature of ceramics), and exit edge chipping (the tool is leaving the workpiece). Ng et al. [18] investigated the effects of the edge chipping under a set of machining conditions with a non-destructive evaluation process. It was reported that no effect has been observed to control the exit chipping due to discontinuity of energy transformation on the interface. Based upon the fracture mechanics theory of Chiu et al. [22], Cao [21] proposed a 2D finite element analysis (FEA) model to predict exit edge chipping size for machining dental ceramics. It was found that crack length, loading orientation, and location are the major variables that determine the size of the exit edge chipping. Yang et al. [23] conducted an experimental study to investigate the mechanisms of edge chipping at elevated temperature in laser assisted milling of silicon nitride ceramics. They concluded that the elevated temperature can significantly reduce edge chipping through softening and toughening mechanisms. Yoshifumi et al. [24] carried out high-precision slot grinding on Mn-Zn ferrites to investigate the chipping mechanism by measuring the chipping size at the slotted edges. It is evident that chipping size can be reduced by decreasing the removal per grain. Wang et al. [25] employed the cutting depth ratio to investigate the effect of uncut chip thickness on groove edge chipping. Their results confirmed that the magnitude of edge chipping is steadily increased with increasing cutting depth ratio. Vogler et al. [26–28] investigated the minimum chip thickness effects on cutting forces in an experimental and numerical way. They observed that the chipping is only formed when the accumulation of cutting thickness is higher than the minimum chipping thickness. Gong et al. [29] developed a comprehensive 3D FEA model of in-process to find the relationship between the distribution of maximum principal stress and edge chipping. They reported that edge chipping can be reduced by optimizing the distribution of the maximum principal stress during the machining process.

Recent studies show that ultrasonic-assisted machining could be a very promising method for machining hard and brittle materials [30–40]. Ahamed et al. [33] conducted a preliminary experimental investigation on the surface and subsurface cracks in rotary ultrasonic machining (RUM) of Al_2O_3 dental ceramics. They concluded that with the assistance of ultrasonic vibration, a better surface quality can be expected for grinding of dental ceramics and subsurface cracks might be significantly reduced. Tesfay et al. [31] conducted a preliminary experimental study on edge chipping in ultrasonic vibration-assisted grinding (UVAG) of bio-ceramic materials. Their results show that UVAG can be a proficient method to reduce edge chipping of bio-ceramic materials. Wang et al. [32] developed a mathematical model for system matching

in UVAG of brittle materials to examine the mechanism of grinding force reduction and surface roughness forming. Based on this mathematical model, they concluded that workpiece surface quality is improved by UVAG. Park et al. [40] performed an experimental study on alumina ceramics to investigate the effect of ultrasonic vibration on surface roughness. In their study, they concluded that ultrasonic assisted machining could reduce the surface roughness from 5 % to 15 %.

Although edge chipping has critical impacts on the long-term performance of bio-ceramics products and on increasing machining costs, very limited studies about it have been reported. It is, therefore, crucial to develop a new cost-effective machining process relevant to control edge chipping in diamond grinding of bio-ceramics. From the literature, it was found that with ultrasonic assisted machining, reduced surface roughness and better surface quality of ceramics materials was obtained [33–40]. One of the main objectives of this paper is to demonstrate the practical use of UVAG in reducing the edge chipping of bio-ceramics materials. In this research, an UVAG system is developed by integrating an ultrasonic vibration generator with a high speed milling machine to evaluate the effect of ultrasonic vibration on edge chippings of bio-ceramics materials.

The present paper is organized into four sections. Following the introduction section, Section 2 addresses the experimental details including experimental setup, experimental conditions and workpiece materials, and experimental measurements. Experimental results and a further experimental validation with Hertzian indentation test are presented and discussed in Section 3. Major conclusions are summarized in Section 4.

2 Experimental details

2.1 Experimental setup

The experimental setup is schematically illustrated in Fig. 2. Figure 2a shows the UVAG system. It mainly consists of a desktop ultra-high speed milling system, an ultrasonic vibration system, and a computer control system. The milling system is used to conduct machining tests for the bio-ceramic workpieces and composed of an ultra-high speed milling machine (Mini-mill J205, Minitech Machinery Corp., Norcross, GA), an air compressor, and a fixture of special design as shown in Fig. 2b. The ultrasonic vibration system includes an ultrasonic generator with two ultrasonic shoe-shape transducers (Sonic Shoe SS902-2, Advanced Sonic Processing Systems, Oxford, CT), which are mounted on the working table of the milling machine through the fixture. The computer control system is employed to control the milling parameters such as tool moving path, feedrate, rotating speed, etc.

A plastic board is mounted in between the working table of the milling machine and the ultrasonic transducers. The two transducers are pressed against the plastic board to activate the

board to vibrate at 20 kHz frequency with vibration amplitude about 2.5 μm . Both transducers are driven in phase and vibrate independently with each other.

2.2 Experimental conditions and workpiece materials

The UVAG process can be found in Fig. 2c and detailed process is illustrated in Fig. 3. From Fig. 2c, three bio-ceramic workpieces (lava, lava partially fired, and alumina 99.5 %) are bonded on the plastic board and vibrate with the board. A diamond tool with metal-bonded diamond abrasives is employed to grind the three workpieces. The workpieces material properties are listed in Table 1.

From Fig. 3, the diamond tool is rotating and fed downwards below the workpiece top surface and then cuts into the workpiece to make a slot. When the ultrasonic vibration is turned off, it becomes a normal grinding process. With the help of the UVAG system, it is easy to investigate the effect of ultrasonic vibration on the process and compare the difference between the UVAG process and the normal grinding process. The bio-ceramic workpieces are indented a distance 6 mm from the edge using a diamond sphere of radius $R=1.5$ mm. The workpieces were rectangular of dimensions of 10 mm (thickness) \times 20 mm (width) \times 30 mm (length) (lava), 10 \times 30 \times 50 mm (alumina), or 15 \times 20 \times 40 mm (lava partially fired). The indentation load p is systematically varied until the chipping was formed. Other detailed experimental conditions can be found from Table 2.

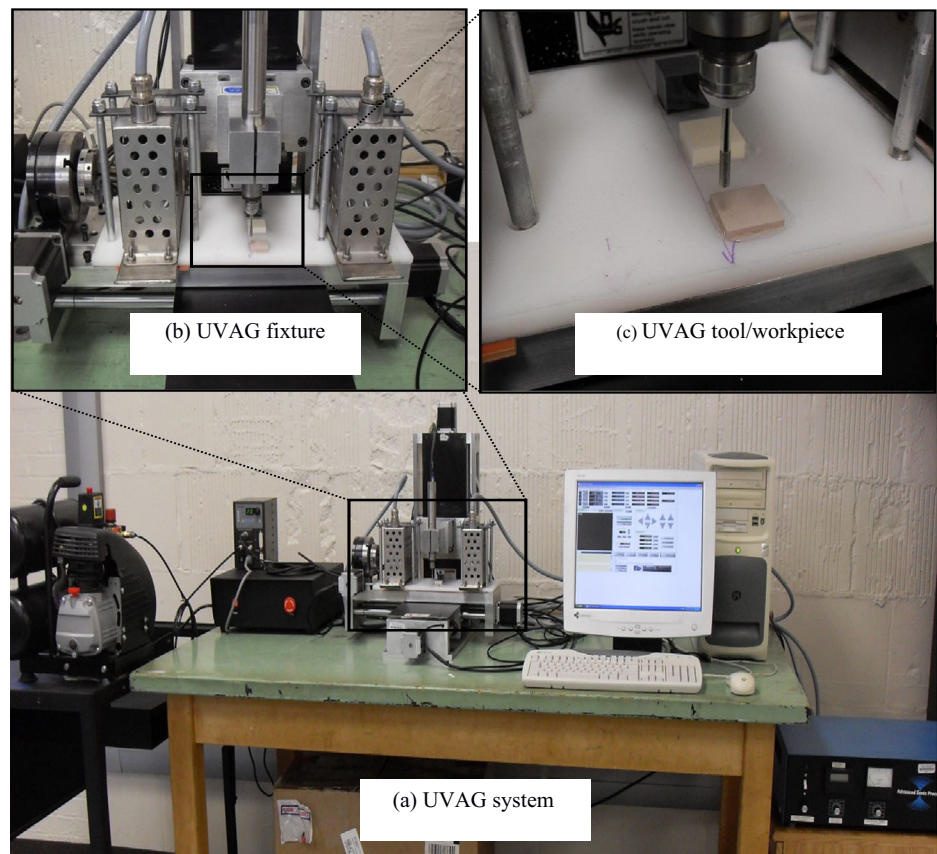
2.3 Experimental measurements

After UVAG and normal diamond grinding tests, the three workpieces are coated in the vacuum chamber of a Polaron SEM Sputter Coater E5400 (Quorum Technologies Ltd., East Sussex, UK) for SEM observation. The SEM observation tests are focused on the machined slots for edge chippings. The observation tests are conducted by using a Hitachi S-3000N PC-controlled SEM (Hitachi High Technologies America, Inc., Pleasanton, CA, USA). Based on the SEM results, the edge chippings size is measured and evaluated as shown as Fig. 4. Eight points around the edge chipping periphery are randomly selected and the distance from the center to the point is measured. The average edge chipping size is then calculated as

$$\Delta L = \frac{\sum_{i=1}^4 (L_i - R)}{8}$$

with 1 standard deviation of

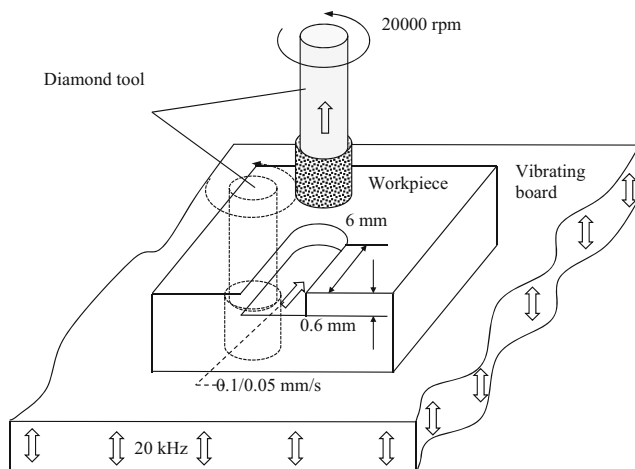
$$\Delta L_{SD} = \sqrt{\frac{\sum_{i=1}^4 (\Delta L_i - \Delta L)^2}{8}}$$

Fig. 2 UVAG system

3 Results and discussion

3.1 Effects of ultrasonic vibration on edge chippings

Figure 5 illustrate the SEM micrograph of edge chippings of the material lava machined by normal diamond grinding and UVAG at equal depth of grinding. It is clear to see that the machined slot quality by UVAG is much better than the normal diamond grinding. For the normal diamond grinding, there exist a lot of edge chippings along the machined slot

**Fig. 3** Illustration of UVAG process

edge and these chippings size varies from ~ 0.3 to ~ 1.2 mm. Most of edge chippings form several continuous areas of chippings along the machined slot. As for UVAG, there are only several tiny edge chippings with size from ~ 0.03 to ~ 0.1 mm that are found along the machine slot edge. Some larger chippings (>0.1 mm) are found near the tool entrance area.

Figure 6 displays the machined SEM micrographs used to quantify edge chipping size. The machined SEM graphs in Fig. 6 show that the chipping size is significantly reduced with the help of ultrasonic vibration. Figure 7 shows the comparison of the average edge chipping size (with error bar of 1 standard deviation) between normal diamond grinding (without ultrasonic vibration) and UVAG (with ultrasonic vibration) for the three bio-ceramic materials. The chipping size is quantified according to the measurement method illustrated in Fig. 4. From Fig. 7, it can be seen that the average edge chipping size produced by normal diamond grinding and UVAG varies from ~ 0.64 to ~ 0.68 mm and from ~ 0.05 to ~ 0.07 mm, respectively, which reveals that with the help of ultrasonic vibration, smaller edge chippings size can be predicted in diamond grinding of bio-ceramic materials. This result is in a very good agreement with the results found by other investigators [21, 23, 24, 31–33].

In all the three figures (Figs. 5, 6, and 7), it is observed that the edge chipping sizes resulted from the UVAG are significantly smaller than the corresponding edge chipping size

Table 1 Workpiece materials properties (lava, lava partially fired, and alumina 99.5 %)

| Property | Unit | Lava | Lava (partially fired) | Alumina 99.5 % |
|----------------------|-------------------|------|------------------------|----------------|
| Young's modulus | Gpa | n/a | n/a | 394 |
| Poisson ration | | n/a | n/a | 0.22 |
| Density | g/cm ³ | 2.5 | 2.3 | 3.7 |
| Tensile strength | MPa | 7 | 20.7 | 260 |
| Compressive strength | MPa | 76.5 | 172.5 | 2070 |
| M-Hardness | | 2 | 6 | 9 |

obtained in conventional grinding process. The possible reasons for the reduction of edge chipping size in the UVAG process is due to the kinematics of the ultrasonic vibration imposed on the grinding process. In UVAG, the tool and workpiece are not in continuous contact due to periodic oscillation of the workpiece as well as superimposed circular movement of the diamond tool [41]. As a result, the contact time, the contact friction, the applied load, and the heat generated in the contact zone are significantly decreased as reported in [41–43]. It has been reported that the superimposed ultrasonic vibration (UVAG) exhibits a high potential for a significant reduction in the cutting force, which directly associates with surface integrity, machining temperature, and machining accuracy [42]. This reduction of load in UVAG may also corresponded to a marked difference in the crack paths generated by the two types of machining, i.e., cracks in the UVAG machining tended to advance slowly toward the edge to produce chips than in the CG machining. Previous research indicated that cutting force is the main influencing parameter on edge chipping as reported by [44] who employed an integrated approach that combines designed experiments and FEM simulations to study edge chipping when drilling advanced ceramics by rotary ultrasonic machining. Their results show that cutting force is the main influencing parameter on edge chipping and conclude that larger edge chipping is almost always accompanied by a higher cutting force. This result is also supported by the evidences observed in many studies [45–47]. In all the three bio-ceramic workpiece materials, the UVAG provides significant advantages over conventional grinding

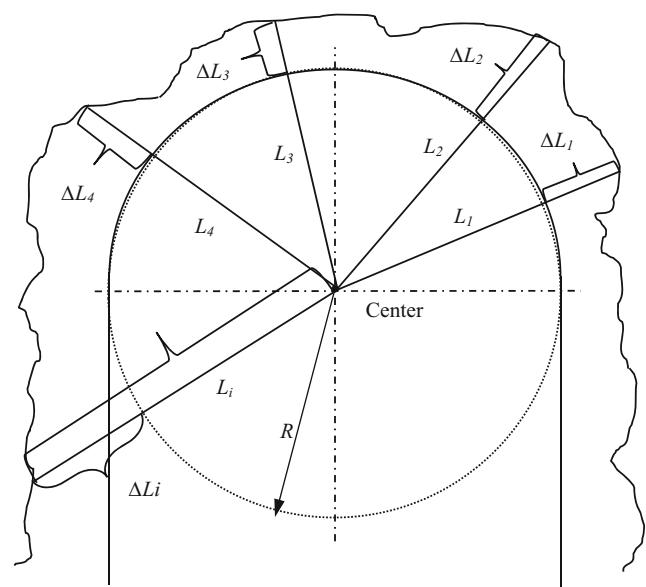
machining operations in reducing size of the edge chipping, which validates the innovation of the designed UVAG method in significantly reducing the edge chipping size of bio-ceramic materials.

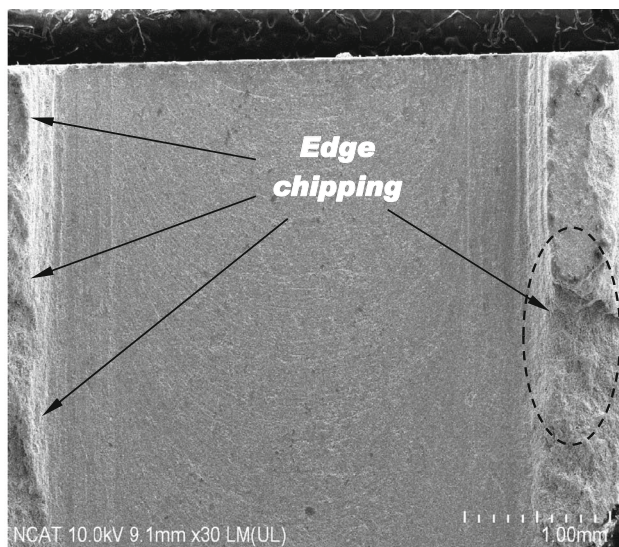
3.2 An indentation test to further verify the effects of ultrasonic vibration

In this section, a Hertzian indentation method with a conical shape diamond indenter was developed and employed to further verify the results of the edge chipping. The Hertzian indentation method is a viable way to test the contact damage that occur in many modern ceramic applications [48]; the failure of components of brittle materials, either by continued ware or erosion, and/or by the introduction of crack-like defects are usually simulated in indentation tests by using hard indenters [49]. Moreover, flaw sizes can be measured by Hertzian indentation [50]. Another great advantage of the Hertzian indentation test include their simplicity, repeatability, suitability, practicality, cost-effectiveness, little experience that is enough for conduction, and can be performed on small specimens [51].

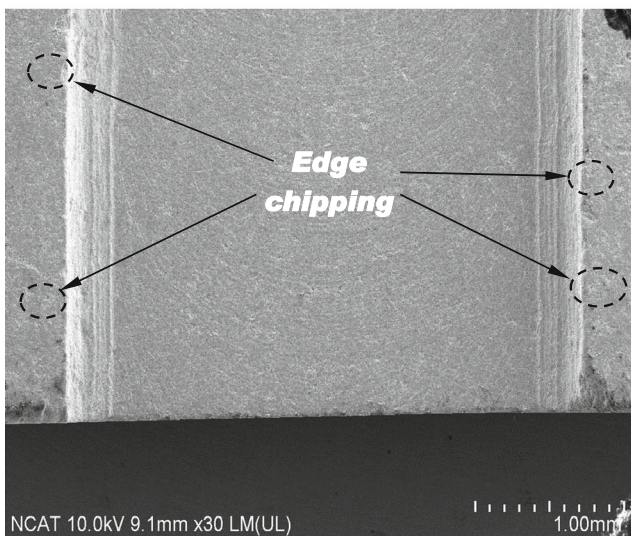
Table 2 Experimental conditions

| Conditions | Specifications |
|------------------------|---|
| Feedrate (mm/s) | Lava: 0.1 Lava partially fired: 0.1 Alumina 99.5 %: 0.05 |
| Spindle speed (rpm) | 20,000 |
| Ultrasonic vibration | Power supply: 50 % Frequency (kHz): 20 Amplitude: $\pm 2.5 \mu\text{m}$ |
| Grinding depth (mm) | 0.6 |
| Grinding distance (mm) | 6 |

**Fig. 4** Measurement of edge chipping size



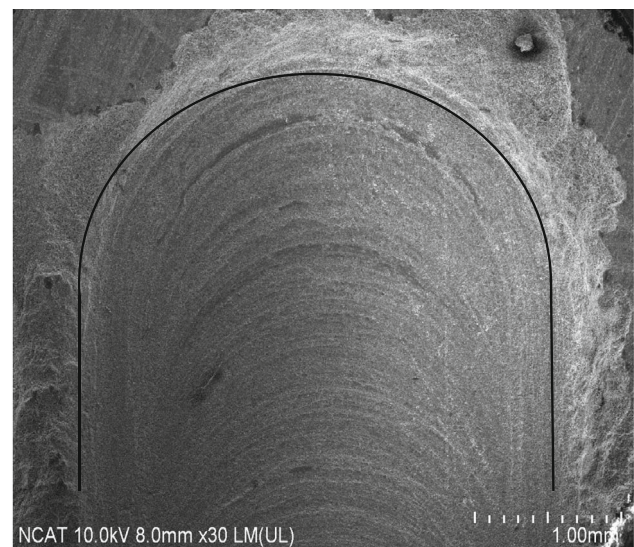
(a) After diamond grinding.



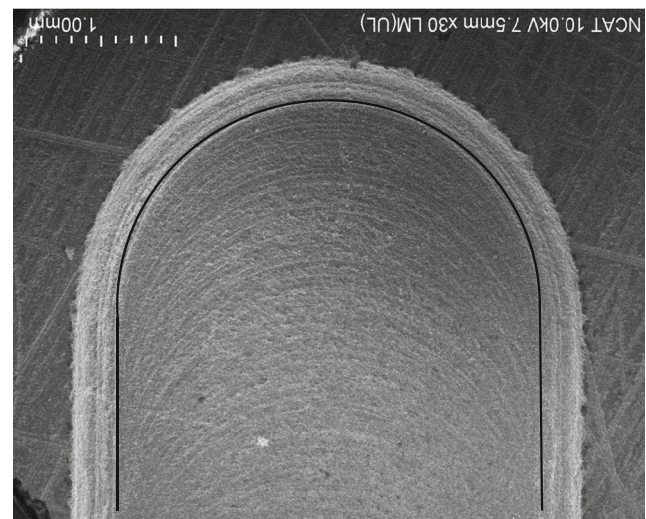
(b) After UVAG.

Fig. 5 SEM micrographs of edge chippings (lava)

Hertzian indentation method has been widely used by many investigators to study edge chipping of brittle materials. Almond and McCormick [52] examined the chipping of various brittle materials loaded with a conical diamond indenter and observed that chips had a constant shape, regardless of the test material and the indentation distance from the edge. A recent study of edge chipping of diamond by spherical indenters [53] found that cracks were not penny shaped and that they did not grow in the direction of the applied force. Chai and Ravinchandran [54] investigated the edge chipping of soda-lime glass by the impact of Vickers and spherical tip cylindrical projectiles. They observed that in the initial stages of damage, blunt indenters developed cone cracks, initiating from the margin of the contact. The mechanism of edge



(a) After diamond grinding.



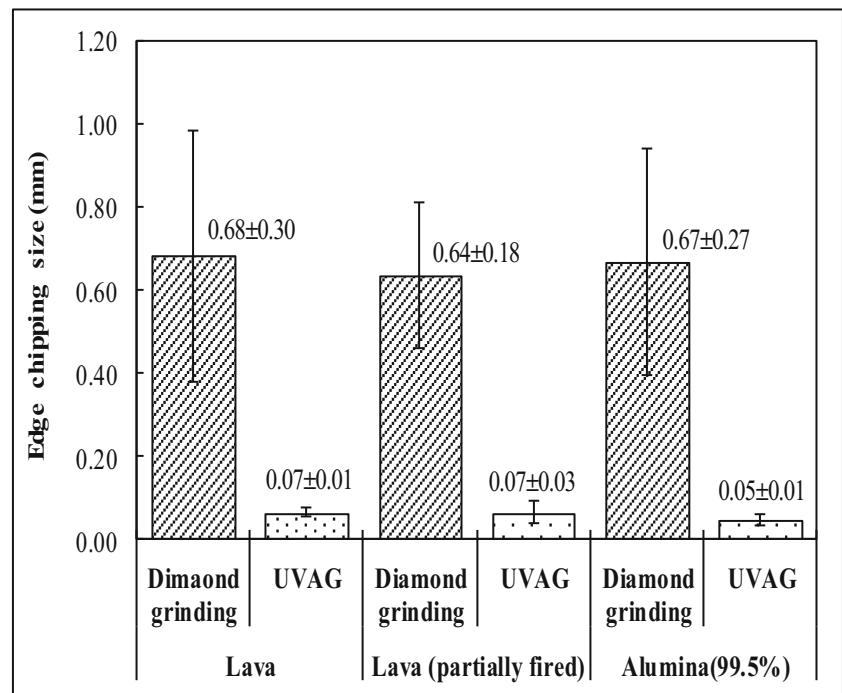
(b) After UVAG.

Fig. 6 Edge chipping measurement under SEM (lava partially fired)

chipping of ceramic by spherical indenter was experimentally investigated [55]. The results showed that the edge chipping was highly sensitive to the indentation distance from the edge, the displacement of the indenter, and the indenter material. It was found that there was an approximately linear relationship between the distance of indentation from the edge and the force required to create a chip. Edge chipping of borosilicate glass by the low velocity impact of freely falling steel and ceramic balls was investigated experimentally using spherical indenters [56]. They found that edge chipping by impact loading required lower forces than by quasi-static loading.

Hertzian indenters induce a wide range of damage mechanisms depending on the indentation distance from the edge,

Fig. 7 Comparison of edge chipping size between diamond grinding and UVAG for three bio-ceramic materials



the indenter material, and the indenter constraint [57]. The indented surface produces axisymmetric Hertzian contact stresses with a maximum tensile stress at the periphery of the contact [58]. At sufficiently high loads, a ring crack is formed which grows to create a Hertzian cone crack. As loading increased, the Hertzian cone cracks propagate asymmetrically to the local distance from the edge. Further increase in the load caused two side cracks to initiate perpendicular to the ring crack. Upon further growth, the side cracks grew to merge with the Hertzian cone crack, forming a single asymmetric cone crack. Although cone cracks are a common feature under spherical indentation, the chipping event is dominated by median-radial cracks [59]. Chai and Ravinchandran [60] observed that in the initial stages of damage, indenters developed cone cracks, initiating from the margin of the contact. As the impact load increased however, the indenters developed median cracks, which grew faster and longer than the initial cone crack. As a result, edge chipping was caused by the extension of penny-shaped median cracks.

Figure 8 shows the schematic illustration of the proposed ultrasonic vibration-assisted Hertzian indentation (UVAI) method. A conical shape diamond indenter is pressed down on the top surface near the edge of the workpiece with a constant feedrate, F , until a chip is formed around the area of contact. The resulted contact area was a shallow circular crack of radius, a , resulting in penetration depth, d , of the indenter into the workpiece. In the ultrasonic vibration-assisted indentation technique, the workpieces were vibrated at amplitude, A , of about $2.5 \mu\text{m}$ with an ultrasonic frequency, f , of approximately 20 kHz, whereas in the common Hertzian

indentation method, the superimposed ultrasonic vibration was turned off. Detailed indentation conditions can be found from Table 2.

Hertzian indentation tests were carried out on three bio-ceramic workpieces (lava, lave partially fired, and alumina 99.5 %). Eight indentation tests were performed for each of the three workpieces, for a total of 24 tests. Half of the tests were performed by UVAI (with ultrasonic vibration) and half were performed by Hertzian indentation (without ultrasonic vibration) under the same condition and configurations. The analysis was done for three indentation depths (1, 1.5, and 2 mm) for both UVAI and Hertzian indentation methods (with

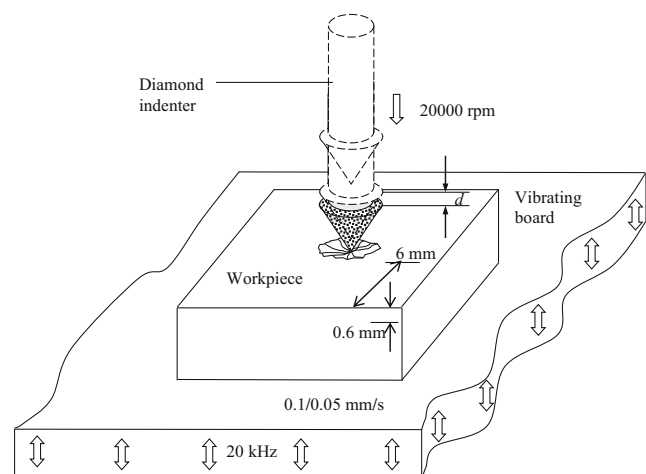
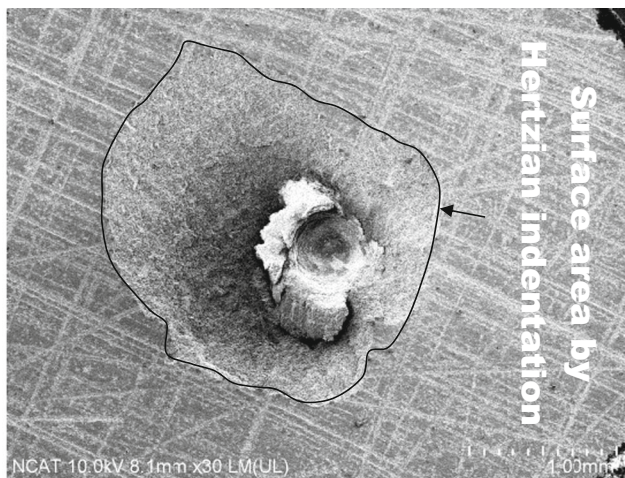


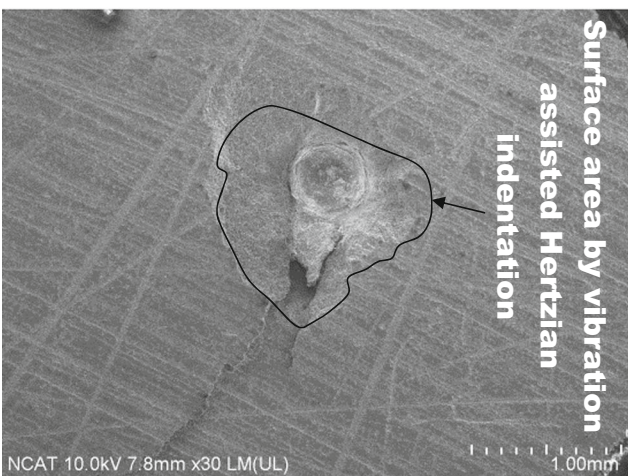
Fig. 8 Systematic illustration of ultrasonic vibration-assisted Hertzian indentation method

and without ultrasonic vibration). To investigate the effect of ultrasonic vibration, the resulted edge chipping surface area were evaluated and compared under scanning electron microscope (SEM).

Figures 9 and 10 depict the SEM micrographs of the bio-ceramic workpieces lava and lava partially fired indented by Hertzian indentation (without ultrasonic vibration) and UVAI (with ultrasonic vibration) under same indentation condition. Figures 9a and 10a illustrate indented edges of workpieces resulted from Hertzian indentation whereas Figs. 9b and 10b show indented edge of workpieces resulted from UVAI tests. As shown in Figs. 9 and 10, the UVAI shows smaller chipping size than the Hertzian indentation method. It is seen that the Hertzian indentation generated thicker, coarse, and longer chips, leading to large edge chipping size and low surface quality while UVAI produced comparatively thin, smooth, and short chips, leading to smaller edge chippings sizes and better surface quality. From these figures, it can be concluded

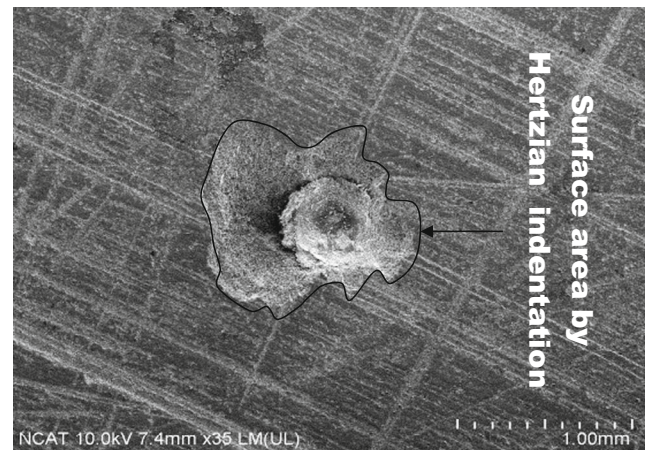


(a) Without Vibration

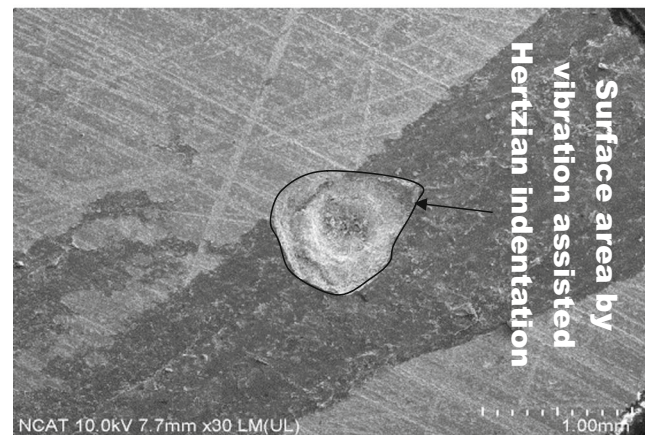


(b) With Vibration

Fig. 9 SEM micrographs of edge chipping (lava) resulted from indentation test: **a** without ultrasonic vibration and **b** with ultrasonic vibration



(a) Without Vibration



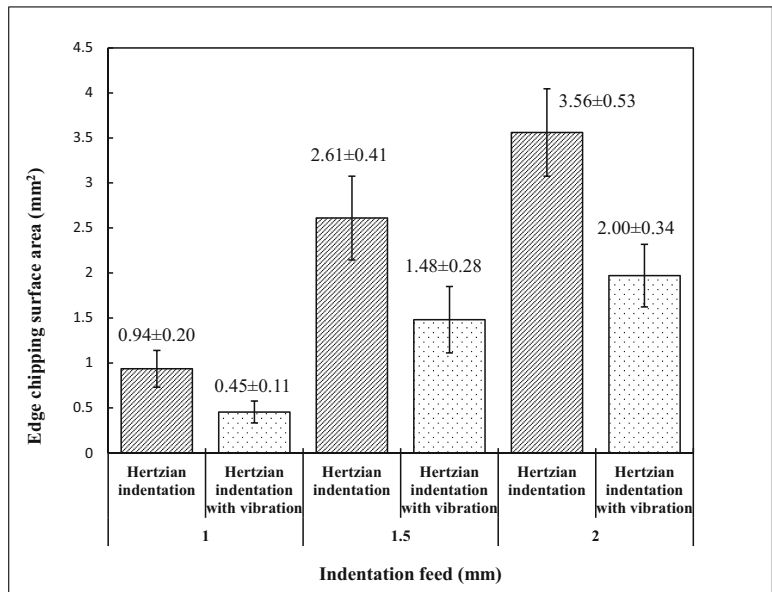
(b) With Vibration

Fig. 10 Edge chipping (lava partially fired) measurement under SEM resulted from indentation test: **a** without ultrasonic vibration and **b** with ultrasonic vibration

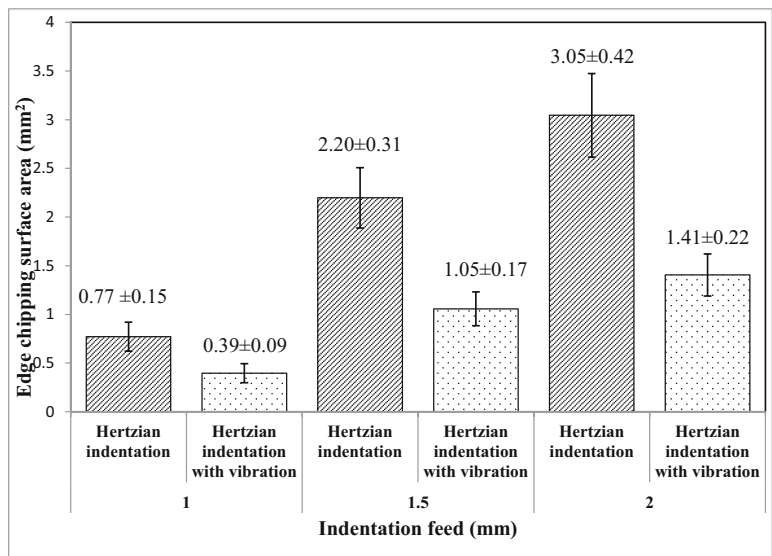
that the chipping size of bio-ceramic materials can be reduced significantly with the aid of ultrasonic vibration. This result is in a very good agreement with results reported in the literature [21, 31–33].

Figure 11 compares the edge chipping size between the Hertzian indentation method (without ultrasonic vibration) method and the UVAI (ultrasonic vibration-assisted Hertzian indentation without ultrasonic vibration) method for three workpiece materials (lava, alumina (99.5 %), and lava partially fired) at different levels of indentation feed. The figure indicates that, at all levels of the indentation feed, the edge chipping sizes resulted from the UVAI is considerably smaller than the corresponding chipping size in Hertzian indentation process. As shown in Fig. 11a, the indented edge surface area for lava in the Hertzian indentation ranges from ~ 0.03 to ~ 5.22 mm^2 with an average mean of ~ 1.00 mm^2 (average mean varying 0.94 – 3.56 mm^2 , see Fig. 11a) and standard deviation (SD) of ~ 1.08 mm^2 , whereas the corresponding chipping size for the UVAI varies from ~ 0.01 to ~ 3.21 mm^2 with a mean of ~ 0.93 mm^2 (average mean varying 0.45 –

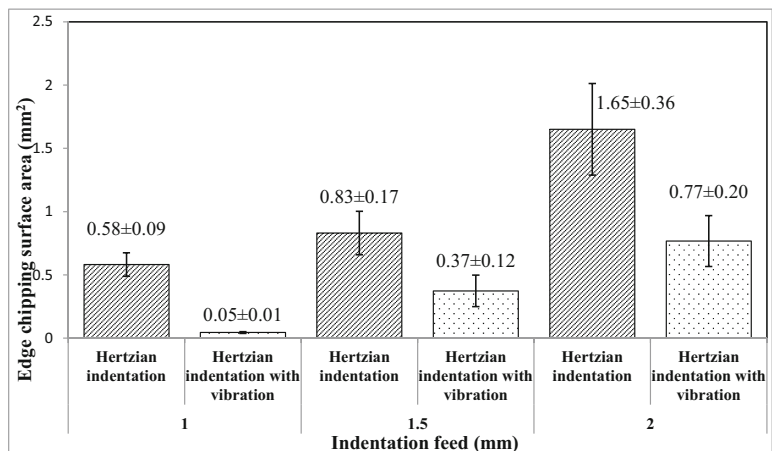
Fig. 11 Comparison of edge chipping size in Hertzian indentation with and without ultrasonic vibration at different levels of indentation feed for three bio-ceramic materials: **a** lava; **b** alumina (99.5 %); and **c** lava partially fired



(a) Lava



(b) Alumina



(c) Lava partially fired

2.00 mm² in Fig. 11a) and SD of ~0.67 mm². Similarly, in Fig. 11b, the indented edge chipping size for alumina workpiece produced by the Hertzian indentation varies from ~0.38 to ~4.34 mm² with a mean of ~2.01 mm² (average mean varying 0.77–3.05 mm²) and SD of ~0.84 mm², while the corresponding edge chipping obtained in the UVAI method extends in size from ~0.006 to ~2.25 mm² with a mean of ~0.34 mm² (average mean varying 0.39–1.41 mm²) and SD of ~0.94 mm². Moreover, the indented edge chipping size for lava partially fired in the Hertzian indentation ranges from ~0.005 to ~1.90 mm² with a mean of ~1.02 mm² (average mean varying 0.58–1.65 mm²) and SD of ~0.60 mm², whereas the corresponding chipping size for the UVAI varies from ~0.009 to ~3.40 mm² with a mean of ~0.34 mm² (average mean varying 0.05–0.77 mm²) and SD of ~0.05 mm² (see Fig. 11c).

In all the three workpiece materials (Figs. 9, 10, and 11), it is evident that the edge chipping sizes resulted from the UVAI are significantly smaller than the corresponding edge chipping size in Hertzian indentation process. The reason for the reduction of edge chipping size in the UVAI may be attributed to the superimposed ultrasonic vibration due to the reduction of load as reported in [61] who conducted indentation tests and finite element simulations, in which an ultrasonic vibration was superimposed at a frequency of 20 kHz to investigate the effects of ultrasonic vibration on the indentation mechanics of Plasticine. They showed that reduction in indentation load is attributed to superimposed ultrasonic vibration as well as the reduction in indentation load may be attributed to a combination of stress superposition and friction reduction, which leads to the reduction of edge chipping size. This result supports the grinding experimental findings deduced in the previous sections (see Fig. 7). The chipping size is reduced on average by ~50 % when the UVAI method is used compared with the Hertzian indentation (see Fig. 11a–c), which obviously indicates the novelty of the UVAI in reducing the edge chipping size of bio-ceramic materials.

4 Concluding remarks

This paper presents an experimental study on the effect of ultrasonic vibration on edge chippings of bio-ceramic materials in UVAG process. Hertzian indentation tests were also employed to further verify the experimental results. Grinding and indentation tests were conducted with and without ultrasonic vibration under the same machining conditions. The following conclusions can be drawn:

- (1) The edge chipping of bio-ceramic materials can be reduced significantly around 10 times smaller with the assistance of ultrasonic vibration.
- (2) UVAG provides significant advantages over normal grinding machining operation in reducing edge

chippings of the bio-ceramics workpieces. In normal grinding, thicker, rough, and longer edge chips with average chipping size varying from ~0.64 to ~0.68 mm can be obtained, whereas in UVAG, comparatively thin, smooth, and shorter chips with average chipping size ranging from ~0.05 to ~0.07 mm were found. Similar results can be found from Hertzian indentation tests.

- (3) The good match of the grinding experimental and Hertzian indentation test results suggest that the developed UVAG system can be considered as a promising and reliable approach to control (or reduce) edge chipping of bio-ceramic materials.

Acknowledgments This work was supported by the National Science Foundation through the CAREER Award CMMI-0953502. The authors also would like to gratefully extend their acknowledgements to Mr. Mark Vidaic at Ceramic Products, Inc. (Hackensack, NJ).

References

1. Kuo K, Tsao C (2012) Rotary ultrasonic-assisted milling of brittle materials. *Trans Nonferrous Metals Soc China* 22:s793–s800
2. Thamaraiselvi TV, Rajeswari S (2004) Biological evaluation of bio-ceramic materials—a review. *Trends Biomater Artif Organs* 18(1): 9–17
3. Hench LL (1991) Bio-ceramics: from concept to clinic. *J Am Ceram Soc* 74(7):1487–1510
4. Rebro PA, Shin YC, Incropera FP (2004) Design of operating conditions for crack free laser-assisted machining of mullite. *Int J Mach Tools Manuf* 44:677–694
5. Yin L, Song XF, Song YL, Huang T, Li J (2006) An overview of in vitro abrasive finishing & CAD/CAM of bio-ceramics in restorative dentistry. *Int J Mach Tools Manuf* 46:1013–1026
6. Changa C, Kuob C (2007) An investigation of laser-assisted machining of Al₂O₃ ceramics planning. *Int J Mach Tools Manuf* 47: 452–461
7. Liu D, Cong WL, Pei ZJ, Tang YJ (2012) A cutting force model for rotary ultrasonic machining of brittle materials. *Int J Mach Tools Manuf* 52:77–84
8. DeAza AH, Chevalier J, Fantozzi G, Schehlb M, Torrecillas R (2002) Crack growth resistance of alumina, zirconia and zirconia toughened alumina ceramics for joint prostheses. *Biomaterials* 23(1):937–945
9. Martin A (2000) Inert bio-ceramics (Al₂O₃, ZrO₂) for medical application. *Injury, Int J Care Injured* 31:S-D33–S-D36
10. Li Y, Qiao G, Jin Z (2002) Machinable AL₂O₃/BN composite ceramics with strong mechanical properties. *Mater Res Bull* 37:1401–1409
11. Weisse B, Affolter C, Terrasi GP, Piskoty G, Köbel S (2009) Failure analysis of in vivo fractured ceramic femoral heads. *Eng Fail Anal* 16(4):1188–1194
12. Willmann G (2002) Bio-ceramics in joint replacement: state-of-the-art and future options. *Ceram Forum Int* 79(5):E27–E31
13. Black J (2005) Bearing surfaces. In: *Ceramics in orthopaedics, Proceedings of the Tenth International BIOLOX Symposium*, Darmstadt, Germany, 3–8
14. Esquivel-Upshaw JF, Anusavice KJ, Young H, Jones J, Gibbs C (2004) Clinical performance of a lithia disilicate-based core ceramic for three-unit posterior FPDs. *Int J Prosthodont* 17(4):469–75

15. Rekow ED, Thompson VP (2005) Near-surface damage—a persistent problem in crowns obtained by computer-aided design and manufacturing. *Proc Inst Mech Eng H: J Eng Med* 219(4):233–243
16. Ting HT, Abou-EL-Hossein KA, Chua HB (2009) Review of micromachining of ceramics by etching. *Trans Nonferrous Met Soc China* 19:s1–s16
17. Chai H (2011) On the mechanics of edge chipping from spherical indentation. *Int J Fract* 169(1):85–95
18. Ng S, Le D, Tucker S, Zhang G (1996) Control of machining induced edge chipping on glass ceramics, In: *Proceedings of the ASME International Mechanical Engineering Congress and Exposition, Atlanta, GA, USA*, 229–236
19. Chai H, Lee JW, Lawn BR (2011) On the chipping and splitting of teeth. *J Mech Behav Biomed Mater* 4:315–321
20. Constantino PJ, Lee JJW, Chai H, Zipfel B, Ziscovici C, Lawn BR, Lucas PW (2010) Tooth chipping can reveal the diet and bite forces of fossil hominins. *Biol Lett* 6:826–829
21. Cao YQ (2001) Failure analysis of exit edges in ceramic machining using finite element analysis. *Eng Fail Anal* 8(4):325–338
22. Chiu WC, Thouless MD, Endres WJ (1998) An analysis of chipping in brittle materials. *Int J Fract* 90:287–298
23. Yang B, Shen X, Lei S (2009) Mechanisms of edge chipping in laser-assisted milling of silicon nitride ceramics. *Int J Mach Tools Manuf* 49(3–4):334–350
24. Yoshifumi O, Tetsuo M, Minoru S (1995) Chipping in high precision slot grinding of Mn–Zn ferrite. *Ann CIRP* 44(1):273–277
25. Wang J-JJ, Liao Y-Y, Huang C-Y (2011) The effect of uncut chip thickness on edge chipping and wheel performance in groove grinding of single crystal silicon. *Proc Inst Mech Eng B J Eng Manuf* 225(8):1255–1262
26. Vogler MP, DeVor RE, Kapoor SG (2004) On the modeling and analysis of machining performance in micro end milling, Part I: surface generation. *J Manuf Sci Eng* 126:685–694
27. Vogler MP, DeVor RE, Kapoor SG (2004) On the modeling and analysis of machining performance in micro end milling, Part II: cutting force prediction. *J Manuf Sci Eng* 126:695–705
28. Vogler MP, DeVor RE, Kapoor SG (2003) Microstructure-level force prediction model for micro milling of multiphase materials. *J Manuf Sci Eng* 125:202–209
29. Gong H, Fang FZ, Zhang XF, Du J, Hu XT (2013) Study on the reduction strategy of machining-induced edge chipping based on finite element analysis of in-process workpiece structure. *J Manuf Sci Eng* 135(1):10
30. Churi NJ, Pei ZJ, Treadwell C (2006) Rotary ultrasonic machining of titanium alloy: effects of machining variables. *J Mach Sci Technol* 10(3):301–321
31. Tesfay HD, Xie Y, Xu Z, Yan B, Li Z C (2013) “An Experimental Study on Edge Chipping in Ultrasonic Vibration Assisted Grinding of Bio-Ceramic Materials”, *Proceedings of the ASME 2013 International Manufacturing Science and Engineering Conference, Madison, Wisconsin, USA.*, pp. V001T01A045, doi:10.1115/MSEC2013-1188
32. Wang Y, Lin B, Wang S, Cao X (2014) Study on the system matching of ultrasonic vibration assisted grinding for hard and brittle materials processing. *Int J Mach Tool Manuf* 77:66–73
33. Ahmed Y, Cong WL, Stanco MR, Xu ZG, Pei ZJ, Treadwell C, Zhu YL, Li ZC (2012) Rotary ultrasonic machining of alumina dental ceramics: a preliminary experimental study on surface and subsurface damages. *J Manuf Sci Eng* 134(6):064501–1
34. Gong H, Fang FZ, Hu XT (2010) Kinematic view of tool life in rotary ultrasonic side milling of hard and brittle materials. *Int J Mach Tool Manuf* 50(3):303–307
35. Akbari J, Borzoei H, Mamduhi MH (2008) Study on ultrasonic vibration effects on grinding process of alumina ceramic (Al₂O₃). *World Acad Sci Eng Technol* 41:785–789
36. Zeng WM, Li ZC, Pei ZJ, Treadwell C (2005) Experimental observation of tool wear in rotary ultrasonic machining of advanced ceramics. *Int Mach Tool Manuf* 45(12–13):1468–1473
37. Tawakoli T, Azarhoushang B (2009) Ultrasonic assisted dry grinding of 42CrMo4. *Int J Adv Manuf Technol* 42(9–10):883–891
38. Singh R, Khamba JS (2007) Taguchi technique for modeling material removal rate in ultrasonic machining of titanium. *Mater Sci Eng A*(460–461):365–369
39. Guzzo PL, Shinohara AH, Raslan AA (2004) A comparative study on ultrasonic machining of hard and brittle materials. *J Braz Soc Mech Sci Eng XXVI*(1):56–61
40. Park KH, Hong YH, Kim KT, Lee SW, Choi HZ, Choi YJ (2014) Understanding of ultrasonic assisted machining with diamond grinding tool. *Mod Mech Eng* 4:1–7
41. Uhlmann E, Spur G (1998) Surface formation in creep feed grinding of advanced ceramics with and without ultrasonic assistance. *CIRP Ann Manuf Technol* 47(1):249–252. doi:10.1016/S0007-8506(07)62828-5
42. Lv D, Huang Y, Wang H, Tang Y, Wu X (2013) Improvement effects of vibration on cutting force in rotary ultrasonic machining of BK7 glass. *J Mater Process Technol* 213(9):1548–1557. doi:10.1016/j.jmatprotec.2013.04.001
43. Zhou Y, Funkenbusch PD, Quesnel DJ (1997) Stress distributions at the abrasive-matrix interface during tool wear in bound abrasive grinding—a finite element analysis. *Wear* 209(1–2): 247–254. Doi:10.1016/S0043-1648(96)07490-X
44. Yue J, Liu WJ, Pei ZJ, Xin XJ, Treadwell C (2004) Study on edge chipping in rotary ultrasonic machining of ceramics: an integration of designed experiments and finite element method analysis. *J Manuf Sci Eng* 127(4):752–758. doi:10.1115/1.2034511
45. Li ZC, Cai LW, Pei ZJ, Treadwell C (2006) Edge-chipping reduction in rotary ultrasonic machining of ceramics: finite element analysis and experimental verification. *Int J Mach Tools Manuf* 46(12–13):1469–1477
46. Zeng WM, Li ZC, Pei ZJ, Treadwell C (2005) Experimental observation of tool wear in rotary ultrasonic machining of advanced ceramics. *Int J Mach Tools Manuf* 45(12–13):1468–1473
47. Ahmed Y, Cong WL, Stanco MR, Xu ZG, Pei ZJ, Treadwell C, Zhu YL, Li ZC (2012) Rotary ultrasonic machining of alumina dental ceramics: a preliminary experimental study on surface and subsurface damages. *J Manuf Sci Eng ASME* 133:064501–1–5
48. Baig MS, Dowling AH, Fleming GJP (2013) Hertzian indentation testing of glass-ionomer restoratives: a reliable and clinically relevant testing approach. *J Dent* 41(11):968–973
49. Seshadri SG, Srinivasan, M (1984) Hertzian fracture testing of ceramics. *Ceram Eng Sci Proc Am Ceram Soc, Volume 5*
50. Roberts SG, Franco A Jr (2004) Surface mechanical analyses by Hertzian indentation. *Cerâmica* 50:94–108
51. Bisrat Y, Roberts SG (2000) Residual stress measurement by Hertzian indentation. *Mater Sci Eng A*288:148–153
52. Almond EA, McCormick NJ (1986) Constant-geometry edge-flaking of brittle materials. *Lett Nat* 321:53–55
53. Zaayman E, Morrison G, Field JE (2009) Edge flaking in diamond. *Int J Refract Met Hard Mater* 27:409–416
54. Chai H, Ravichandran G (2009) On the mechanics of fracture in monoliths and multilayers from low-velocity impact by sharp or blunt-tip projectiles. *Int J Impact Eng* 36:375–385
55. Mohajerani A, Spelt JK (2010) Edge chipping of borosilicate glass by blunt indentation. *Mech Mater* 42(12):1064–1080
56. Mohajerani A, Spelt JK (2011) Edge chipping of borosilicate glass by low velocity impact of spherical indenters. *Mech Mater* 43(11): 671–683
57. Mohajerani A, Spelt JK (2010) Edge chipping of borosilicate glass by blunt indenters. *Mech Mater* 2010(42):1064–1080

58. Mohajerani A, Spelt JK (2011) Edge chipping of borosilicate glass by low velocity impact of spherical indenters. *Mech Mater* 43(11): 671–683. doi:[10.1016/j.mechmat.2011.06.016](https://doi.org/10.1016/j.mechmat.2011.06.016)
59. Cha H (2011) On the mechanics of edge chipping from spherical indentation. *Int J Fract* 169(1):85–95. doi:[10.1007/s10704-011-9589-7](https://doi.org/10.1007/s10704-011-9589-7)
60. Chai H, Ravinchandran G (2009) On the mechanics of fracture in monoliths and multilayers from low-velocity impact by sharp or blunt-tip projectiles. *Impact Eng* 2009(36):375–385
61. Huang Z, Lucas M, Adams MJ (2001) Effect of ultrasonic vibration on wedge indentation of a model elasto-viscoplastic material. In: *Proceedings of the Society of Photo-Optical Instrumentation Engineers (SPIE) 3rd International Conference on Experimental Mechanics*, Beijing, China, pp. 445–448. (doi:[10.1117/12.468766](https://doi.org/10.1117/12.468766))